PRAMANA — journal of physics

Vol. 84, No. 6
June 2015
pp. 1023–1032

Quantum confinement effects in low-dimensional systems

D TOPWAL
Institute of Physics, Sachivalaya Marg, Sainik School P.O., Bhubaneswar 751 005, India
E-mail: dinesh.topwal@iopb.res.in

DOI: 10.1007/s12043-015-0999-3; ***e*Publication:** 3 June 2015

Abstract. The confinement effects of electrons in ultrathin films and nanowires grown on metallic and semiconducting substrates investigated using band mapping of their electronic structures using angle-resolved photoemission spectroscopy is discussed here. It has been shown that finite electron reflectivity at the interface is sufficient to sustain the formation of quantum well states and weak quantum well resonance states even in closely matched metals. The expected parabolic dispersion of *sp*-derived quantum well states for free-standing layers undergoes deviations from parabolic behaviour and modifications due to the underlying substrate bands, suggesting the effects of strong hybridization between the quantum well states and the substrate bands. Electron confinement effects in low dimensions as observed from the dispersionless features in the band structures are also discussed.

Keywords. Confinement; quantum well states; ARPES.

PACS Nos 73.21.Fg; 79.60.Dp

1. Introduction

When the size of the enclosure trapping electrons is of similar dimension as that of the Fermi wavelength associated with them, electrons feel the effect of confinement. Such confinement leads to the quantization of energy levels and can give rise to modifications of their thermal, electronic, optical, magnetic properties, etc. which can be distinctively different from their bulk or unconfined counterparts. These confinement effects gave rise to new fields of research such as, nanoscience and nanotechnology, which offer an ample playground for low-dimension physics. In this review article the focus is on ultrathin films where confinement of electrons in films can give rise to standing-wave-like quantum well states. Reasons for such confinement and the interaction of the quantum well states (QWS) with the substrate bands is discussed. We also discuss an example of one-dimensional confinement of electrons in nanowires and the effect of dimensionality on the density-of-states.

2. Two-dimensional confinement

Ultrathin films with thicknesses of a few atomic layers are good candidates for confining electrons in two dimensions. Here the motion of electrons perpendicular to the surface of the film can be constrained, provided the energy and momentum states of the substrate and the thin film do not overlap. The surface and interface potentials of an ultrathin film can then behave like the reflecting walls of a two-dimensional quantum well for the electron waves; a situation analogous to a particle-in-a-box picture of elementary quantum mechanics and will give rise to a series of discrete quantum well electronic states [1]. The degree of localization of electrons within the energy levels of the thin film layer is defined by their hybridization with the substrate wave functions. Fully localized QWS form in the film if the electron energy corresponds to the energy gap of the substrate band structure, like in semiconductor superlattices, where the fundamental gaps of semiconductors plays the role of a barrier for the carrier confinement [2–4]. However, a partial electron confinement in metallic films can be attained to various degrees depending on the matching conditions between the film and the substrate states [1,5]. In the following subsections, two examples are considered where the role of substrates in confinement and their effects on the QWS are discussed.

2.1 *Electron confinement in closely matched metals: Au/Ag(1 1 1)*

Au and Ag are two metals in the periodic table that have the same crystal structure, nearly perfectly matched lattices, and very similar band structures. Figure 1 shows Au and Ag bulk band structure for the normal emission for Au(1 1 1) and Ag(1 1 1) along which *sp* QWS or quantum well resonance states (QWRS) are expected. Top of the Au *sp* band is at around 1.1 eV binding energy (marked by horizontal dashed line) compared to 0.3 eV for Ag. Along this particular direction and in this very small energy range, for Ag electrons Au behaves like a semiconductor and can support a set of quantized states [6,7]. In the rest of the energy range, Ag *sp* bands are very similar to those of Au, with a slight offset near the Fermi level to higher energy with respect to the Au states. Hence, QWS are not observed in this region. However, when Au films are deposited on Ag(1 1 1), Au *sp* states practically degenerate everywhere with substrate Ag *sp* states, as can be seen from figure 1. Thus, the Au–Ag system is believed to be one of the worst candidates for the formation of QWS. Photoemission studies of Au films on Ag(1 1 1) carried out way back in 1988 [6], did not observe any QWS or QWRS in the direction normal to (1 1 1) surface and concluded that the Au *sp* electrons cannot be confined in Au films grown on Ag [8]. This was therefore considered to be a classic case where reflectivity across the metal–metal interface is too negligible so that one cannot observe any confinement effects.

With the advancement in detector technology (since 1988), fast two-dimensional band mapping can now be performed by simultaneously collecting intensity images over a wide angle range very efficiently, providing the possibility of revisiting the Au/Ag(1 1 1) system [9]. Figure 2a shows the band dispersions along the $\bar{M}$–$\bar{\Gamma}$–$\bar{K}$ direction for a 12 monolayer (ML) Au film deposited on Ag(1 1 1) substrate using 57 eV photon energy. Apart from the most prominent spectral feature, i.e. Au(1 1 1) Shockley surface state (a parabolic band centred around $\bar{\Gamma}$ just below the Fermi energy), and bands mostly

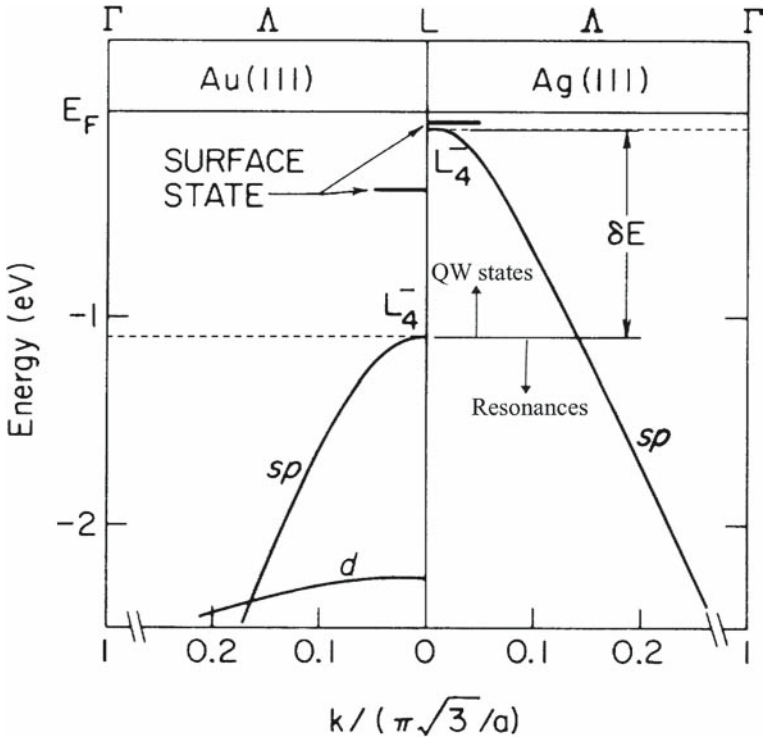

Figure 1. Valence-band dispersion curves for Au(1 1 1) and Ag(1 1 1) along the [1 1 1] direction. For each system, top of the *sp* band (L_4) and surface state is indicated. Energy window δE indicates the region for the formation of QW states of Ag on Au(1 1 1) (reprinted with permission from ref. [6] copyright 2015, by the American Physical Society).

of *d* character beyond 2 eV binding energy, the intensity map displays only very faint features within 2 eV from E_F. These faint features are better visualized in energy distribution curves (EDCs) plotted in figure 2b. Here the normal emission spectrum (marked by black), corresponds to the one reported in [6] and does not display any additional prominent features besides the Shockley surface state. However, a careful examination of the EDCs reveals very weak and broad structures dispersing towards E_F for increasing emission angle for the *sp* states. Further, relatively sharper and well-defined features are observed near the high-symmetry point $\bar{M}$, which are highlighted by green spectra and arrows. The different spectral intensity of the *sp* states in the energy–momentum space suggests that the confinement of electrons in Au film on Ag(1 1 1) occurs to a widely different extent, depending on the electron energy and wave vector. It seems to be higher for the *sp* bands near the $\bar{M}$ Brillouin zone boundary, compared to the rest of the regions.

To enhance the very faint spectral features present in figure 2b, the area enclosed by the EDCs in the binding energy region between 1 and 2 eV is normalized and plotted as the first derivative of the intensity maps in figure 3b. Weaker features that could not be otherwise observed in figure 2a now become clearly visible. The data display a series

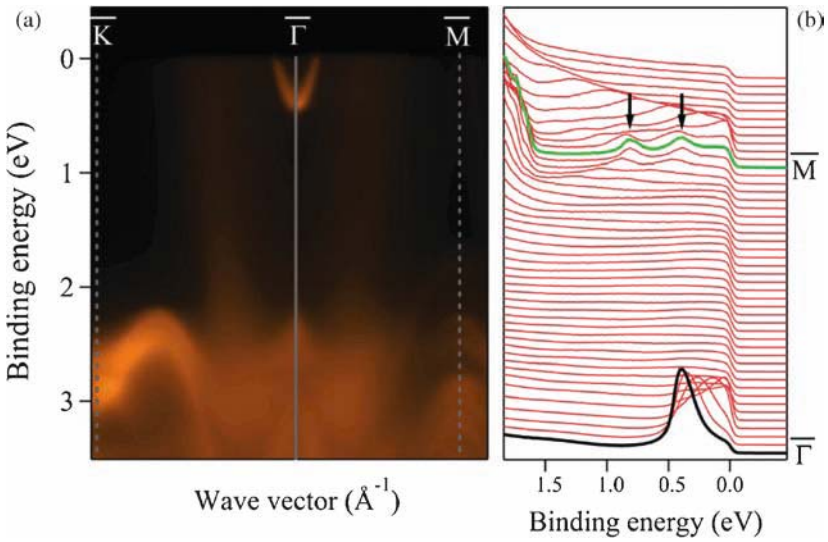

Figure 2. (**a**) Photoemission intensity map as obtained along the $\bar{K}$–$\bar{\Gamma}$–$\bar{M}$ direction for 12 ML Au film deposited on Ag(1 1 1). (**b**) EDCs corresponding to the $\bar{\Gamma}$–$\bar{M}$ direction, plotted after normalizing the area enclosed by EDCs in the binding energy region between 1 and 2 eV. Arrows highlight two prominent, downward dispersing bands (reprinted with permission from ref. [9] copyright 2015, by the American Physical Society).

of dispersive parabolic Au bands about $\bar{\Gamma}$ symmetry direction which can be attributed to QWRS. Observation of these weak QWRS suggests that the electrons are only marginally confined in the Au film over a wide energy–momentum range. One simple test of the quantum size effect is to change the film thickness. As the thickness decreases, the difference between the neighbouring allowed values of k increases and so does the energy difference, hence fewer QWRS are expected for films of lesser thickness. Figure 3a shows QWRS for 7 ML Au film which has lesser number of QWRS than the 12 ML case (figure 3b) as expected. Here too the spectral features in the *sp* electron region are very faint, similar to that for the 12 ML case.

To investigate the origin of the weak spectral features closer to the Fermi level and to understand the reasons for different degrees of confinement in the energy–momentum space, comparison is made between the Bloch spectral function (obtained from density functional theory (DFT) calculations [10–12]) and the corresponding transmission map calculated for an interface between semi-infinite Au and semi-infinite Ag in the (1 1 1) direction as depicted in figures 3c and 3d, respectively [13,14]. Although the Au and Ag band structures are very similar in this energy region and strongly degenerate, the Au/Ag interface does not show perfect transmission $T^2 = 1$. There exists a small but finite electron reflectivity ($R^2 = 1 - T^2$) of about 0.02 which leads to the formation of the experimentally observed weak QWRS. The calculated QWRS bands are also very weakly localized in the Au film, as indicated by the colour code in figure 3c demonstrating the weak confinement. Further, close to $\bar{\Gamma}$ point near the Fermi edge region and at higher energies in the energy–momentum space around $\bar{M}$ and near $\bar{K}$ symmetry points,

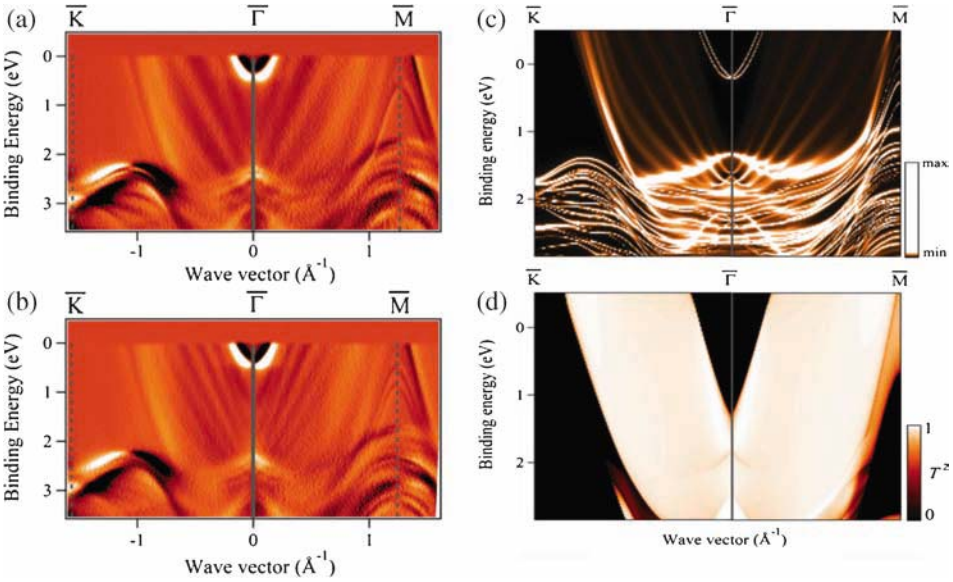

Figure 3. First derivative of the intensity map plotted for (**a**) 7 ML and (**b**) 12 ML of Au film deposited on Ag(1 1 1). (**c**) Bloch spectral function for a 12 ML Au film on semi-infinite Ag(1 1 1) close to the Fermi level. (**d**) Transmission at Ag/Au(1 1 1) interface in the same energy range (reprinted with permission from ref. [9] copyright 2015, by the American Physical Society).

Bloch states are not present in the semi-infinite substrate. These are the regions where the electron reflectivity is very large and explains the formation of prominent Au surface state and sharp and intense feature (indicated in figure 2b) in these gaps. These results hence emphasize that confinement of electrons is a quite general property of metal film and multilayer systems, and the degree of confinement is related to the degree of electronic reflectivity across the interface.

2.2 *Influence of the substrate bands on the QWS*

First-principles electronic structure calculations for free-standing Ag(1 1 1) layers depict *sp*-derived QWS in the proximity of the Fermi level E_F around $\bar{\Gamma}$ symmetry point which can be labelled with principal quantum number n as shown in figure 4a [15]. The n = 1, 2, 3 and 4 states as well as the Shockley surface state, are nearly isotropic about the centre of the surface Brillouin zone, up to 1 eV below E_F. However, states with higher n exhibit less pronounced energy dispersion along $\bar{M}$ than along $\bar{K}$ symmetry point, due to the gap opening at the $\bar{M}$ point in Ag zone boundary. This results in change in the shape of QWS contours from circular shape for lower n values to hexagonal-like shape for higher n values as depicted in figure 4b.

To study the influence of substrate bands on QWS, Ag film was deposited on Ge(1 1 1) [3]. *sp*-derived states of Ag films can be truly confined on Ge(1 1 1) substrate owing to the fundamental gap of the semiconductor. However, the electronic structure of the Ag

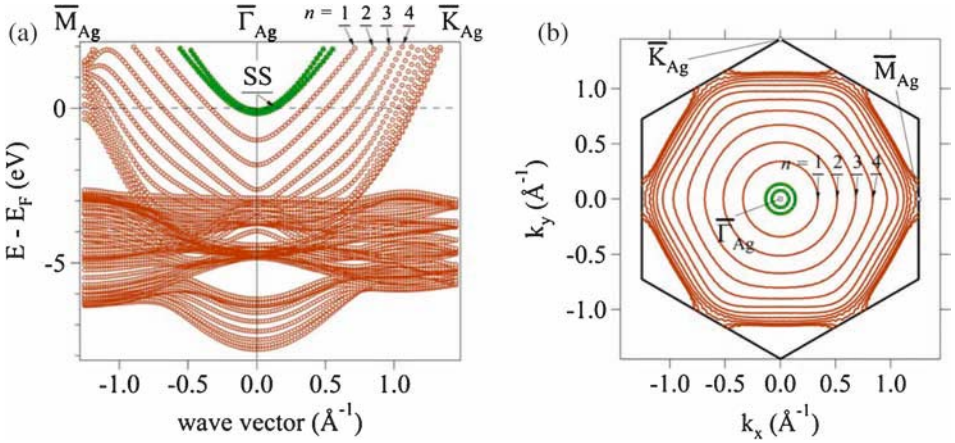

Figure 4. *Ab-initio* calculations of a free-standing 13 ML Ag(1 1 1) film. (**a**) QW band dispersion along the $\bar{M}$–$\bar{\Gamma}$–$\bar{K}$ line. (**b**) *sp*-QW contours at E_F (reprinted with permission from ref. [15] copyright 2015, by the American Physical Society).

film is modified due to the underlying substrate bands [16]. Literature reports point out that the parabolic nature of the QWS is abruptly interrupted by multiple discontinuities in films of Al on Si(1 1 1) [17] and Mg on Mo(1 1 0) [18]. Further, in Cu films on Co(0 0 1) the *sp*-levels bifurcate at certain regions in the energy–momentum space [19]. These observed perturbations to the ground-state electronic structure of the metal layers are explained in terms of symmetry-selective hybridization between the film and the substrate states.

Figure 5a shows certain cuts of the experimentally obtained three-dimensional volume data for 17 ML of Ag film grown on Ge(1 1 1) revealing energy dispersion relation between $E(K_x)$ and $E(K_y)$ high symmetry directions. The spectral features are dominated by near parabolic QWS bands centred about the zone centre $\bar{\Gamma}$. The parabolic nature of the QWS is interrupted by kinks at multiple positions. On careful examination of the intensity map along the $\bar{M}$–$\bar{\Gamma}$–$\bar{K}$ direction, shown in figure 5b, a gap seems to open up between QWS and bands with downward energy dispersion from $\bar{\Gamma}$. Irrespective of the film thickness, three sets of curves are observed in the data which are marked by dashed line in figure 5b and is also represented by full symbols connected by lines in figure 5c. Figure 5c also represents with open symbol the calculated topmost Ge bands labelled as HH (heavy hole), LH (light hole) and SO (split-off) bands [20]. The observed kinks and the calculated bands coincide suggesting that the modifications in the QWS is caused by the hybridization of the Ag electron wave function with those of Ge bands.

Hybridization also results in the modification of the QWS contours as depicted in the sequence of images in figure 6. Focussing on the evolution of $n = 3$ QWS at selected energies, at 0.36 eV below E_F (figure 6a), $n = 3$ QWS appears to be rounded hexagonal which transforms to a clear hexagonal-like energy contour at 0.66 eV below E_F in figure 6b. It turns almost circular in figure 6c and surprisingly, in figure 6d QWS transforms to a hexagonal-like pattern once again but this time rotated in-plane by 30° with

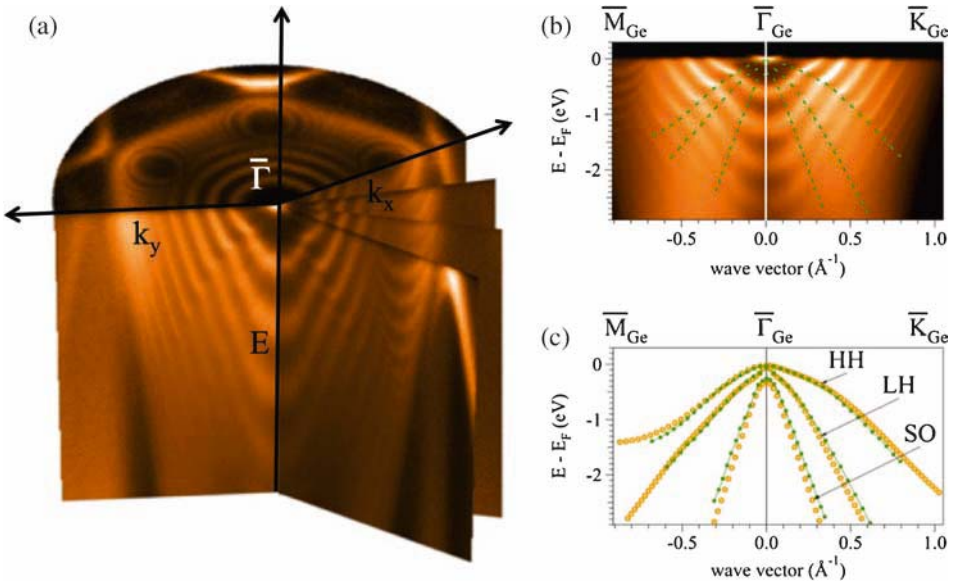

Figure 5. (**a**) Various cuts of the three-dimensional data showing energy vs. momentum dispersion relations for Ag film of 17 ML thickness on Ge(1 1 1). (**b**) Photoemission intensity maps along $\bar{M}$–$\bar{\Gamma}$–$\bar{K}$ direction. (**c**) Substrate bands replotted close to $\bar{\Gamma}$ symmetry point, which are classified as the HH, LH and SO bands. Measured band edges are denoted by full symbols connected by lines while calculated band edges are shown by open symbols. Measured Ge band edges are also shown in (**b**) as dashed lines (reprinted with permission from ref. [15] copyright 2015, by the American Physical Society).

respect to figure 6b. Similar evolution is also seen for $n = 2$ state. To explore the origin of the observed behaviour, dotted lines corresponding to the onset of heavy holes (HH) and light holes (LH) of the Ge band edge are also plotted in the same figure. Overlapping of the QWS contours and Ge band edges clearly explains that the modifications to the QWS is due to its proximity or hybridization with the Ge band edge states [15,16].

3. One-dimensional confinement

For confining electrons in one-dimension, systems need to be chosen and prepared accordingly. One such system is silicon nanowires grown on Ag(1 1 0). Figure 7a shows the scanning tunnelling microscopy (STM) image of Si nanowires which arrange themselves in a densely packed regular arrangement. These nanowires are 1 ML thick and have a width of about 2 nm [21]. In this arrangement, electrons of Si are free to move only along the length of the nanowires, i.e. along [$\bar{1}$ 1 0] direction, while their motion along the other two directions, i.e. along [0 0 1] and [1 1 0] directions (normal to the surface of the substrate) is restricted. The effect of such a confinement on the electronic structure or band structure is studied via angle-resolved photoemission spectroscopy. Figures 7c and 7d

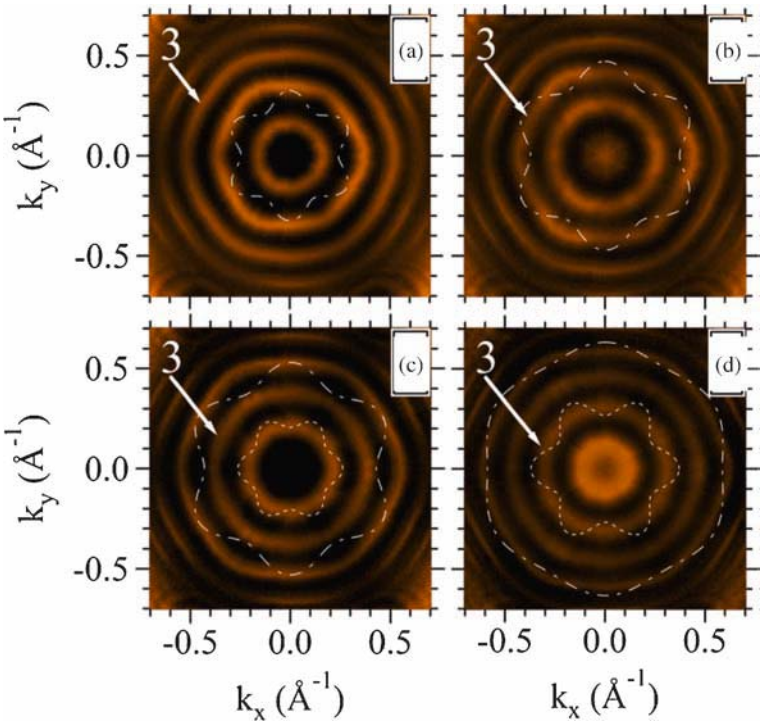

Figure 6. Constant energy cuts of the electronic structure of a 17 ML Ag film grown on Ge(1 1 1). The $n = 3$ QW contour appears to be a rounded hexagon at $E_F = 0.36$ eV (**a**), clearly hexagonal at $E_F = 0.66$ eV (**b**), round at $E_F = 0.81$ eV (**c**) and again hexagonal-like at $E_F = 1.11$ eV (**d**). The symmetry axes of the hexagonal-like QW contours in (**b**) and (**d**) are clearly rotated by 30° with respect to each other. Dash–dotted and dotted lines in (**a**)–(**d**) indicate the onset of the heavy hole and light hole Ge band edges, respectively, as described in the text (reprinted with permission from ref. [15] copyright 2015, by the American Physical Society).

represent band dispersions measured using 78 eV photon energy along and perpendicular to the length of the nanowire, i.e. along $[\bar{1}\,1\,0]$ and $[0\,0\,1]$ directions, respectively. In the direction perpendicular to the nanowires, where there is confinement, dispersionless band behaviour is indicated by S2, S3 and S4 in figure 7d, while along the length of the nanowires, where there is no confinement, highly dispersive π and π^* bands of Si are observed as seen in figure 7c [21]. Modifications to the electronic structure due to one-dimensional confinement is also visible in the constant energy contours as shown in figure 7b, where vertical lines are observed along the length of the nanowires where Si electrons are free to move, but their horizontal motion is restricted due to confinement effects.

Apart from the one-dimensional confinement effects, the Si/Ag(1 1 0) system has pronounced similarities to graphene, where both the systems consist of single monolayers with hexagonal arrangement of atoms [22,23] and is termed as Silicine [24]. Band dispersions along the length of the Si nanowires show linearly dispersing π and π^* bands close

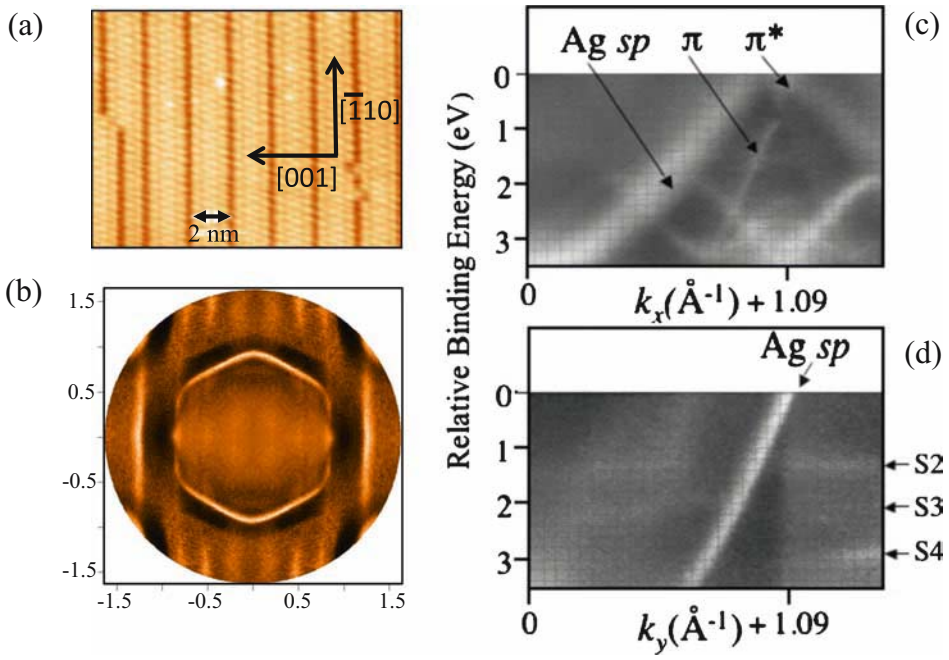

Figure 7. (**a**) STM image of the dense array of Si nanowires forming a 1D grating with a pitch of ∼2 nm. (**b**) Constant energy cuts at $E_F = 1.5$ eV through the electronic structure of Si nanowires grown on Ag(1 1 0). Band dispersion for the array of Si nanowires (**c**) along the length of nanowires (**d**) perpendicular to the nanowires (Figures 7a, 7c, 7d reprinted with permission from ref. [21], copyright 2015, AIP Publishing LLC, while figure 7b © IOP Publishing. Reproduced with permission from ref. [25]. All rights reserved.)

to E_F at $\bar{X}$ point [21], having close analogy with the π and π^* bands of graphene forming the Dirac cones.

Acknowledgements

The author gratefully acknowledges Dr C Carbone and all his group members at VUV beam line, Elettra Synchrotron Light Source, Italy where all the experiments were performed and International Centre for Theoretical Physics (ICTP), Trieste, Italy for the TRIL fellowship.

References

[1] T-C Chiang, *Surf. Sci. Rep.* **39**, 181 (2000)
[2] I Matsuda, T Ohta and H W Yeom, *Phys. Rev. B* **65**, 085327 (2002)
[3] S-J Tang, L Basile, T Miller and T-C Chiang, *Phys. Rev. Lett.* **93**, 216804 (2004)
[4] S-J Tang, W-K Chang, Y-M Chiu, H-Y Chen, C-M Cheng, K-D Tsuei, T Miller and T-C Chiang, *Phys. Rev. B* **78**, 245407 (2008)

[5] W E McMahon, T Miller and T-C Chiang, *Phys. Rev. B* **54**, 10800 (1996)
[6] T Miller, A Samsavar, G E Franklin and T-C Chiang, *Phys. Rev. Lett.* **61**, 1404 (1988)
[7] Li Huang, X G Gong, E Gergert, F Forster, A Bendounan, F Reinert and Zhenyu Zhang, *Europhys. Lett.* **78**, 57003 (2007)
[8] F J Palomares, M Serrano, A Ruiz, F Soria, K Horn and M Alonso, *Surf. Sci.* **513**, 283 (2002)
[9] D Topwal, U Manju, D Pacil, M Papagno, D Wortmann, G Bihlmayer, S Blgel and C Carbone, *Phys. Rev. B* **86**, 085419 (2012)
[10] For a programme description see http://www.flapw.de
[11] E Wimmer, H Krakauer, M Weinert and A J Freeman, *Phys. Rev. B* **24**, 864 (1981)
[12] D Wortmann, H Ishida and S Blügel, *Phys. Rev. B* **66**, 075113 (2002)
[13] P Moras, D Wortmann, G Bihlmayer, L Ferrari, G Alejandro, P H Zhou, D Topwal, P M Sheverdyaeva, S Blugel and C Carbone, *Phys. Rev. B* **82**, 155427 (2010)
[14] Y Imry and R Landauer, *Rev. Mod. Phys.* **71**, S306 (1999)
[15] P Moras, D Topwal, P M Sheverdyaeva, L Ferrari, J Fujii, G Bihlmayer, S Blgel and C Carbone, *Phys. Rev. B* **80**, 205418 (2009)
[16] Y Liu, N J Speer, S-J Tang, T Miller and T-C Chiang, *Phys. Rev. B* **78**, 035443 (2008)
[17] L Aballe, C Rogero, P Kratzer, S Gokhale and K Horn, *Phys. Rev. Lett.* **87**, 156801 (2001)
[18] A M Shikin and O Rader, *Phys. Rev. B* **76**, 073407 (2007)
[19] Eli Rotenberg, Y Z Wu, J M An, M A Van Hove, A Canning, L W Wang and Z Q Qiu, *Phys. Rev. B* **73**, 075426 (2006)
[20] D A Papconstantopolous, *Handbook of the band structure of elemental solids* (Plenum, New York, 1986)
[21] P De Padova, C Quaresima, C Ottaviani, P M Sheverdyaeva, P Moras, C Carbone, D Topwal, B Olivieri, A Kara, H Oughaddou, B Auffray and G Le Lay, *Appl. Phys. Lett.* **96**, 261905 (2010)
[22] B Aufray, A Kara, S Vizzini, H Oughaddou, C Landri, B Ealet and G Le Lay, *Appl. Phys. Lett.* **96**, 183102 (2010)
[23] G Le Lay, B Aufray, C Landri, H Oughaddou, J P Biberian, P De Padova, M E Davila, B Ealet and A Kara, *Appl. Surf. Sci.* **256**, 524 (2009)
[24] P Vogt, P De Padova, C Quaresima, J Avila, E Frantzeskakis, M Carmen Asensio, A Resta, B Ealet and G L Lay, *Phys. Rev. Lett.* **108**, 155501 (2012)
[25] P De Padova, P Perfetti, B Olivieri, C Quaresima, C Ottaviani and G Le Lay, *J. Phys. Condens.*: *Matter* **24**, 223001 (2012)